Soft Matter

Accepted Manuscript

ROYAL SOCIETY OF CHEMISTRY

www.rsc.org/softmatter

Relationship between Particle Elasticity, Glass Fragility, and Structural Relaxation in Dense Microgel Suspensions

Raymond P. Seekell, III, [1] Prasad S. Sarangapani[1], Zexin Zhang[2], and Yingxi Zhu[1,*]

1. Chemical and Biomolecular Engineering, University of Notre Dame, Notre Dame, IN 46556, USA

2. Center for Soft Condensed Matter Physics and Interdisciplinary Research, Soochow University, Suzhou 215006, China

* Corresponding email: yzhu3@nd.edu

Abstract

"Fragile" glassy materials, which include most polymeric materials and organic liquids, exhibit a steep and super-Arrhenius dependence of relaxation time with temperature upon the glass transition and have been extensively studied. Yet, a full understanding of strong glass formers that exhibit an Arrhenius dependence on temperature is still lacking. In this work, we have investigated the glassy dynamics of Poly(N-isopropylacrylamide) (PNIPAM) microgel particles of varied elasticity in dense aqueous suspensions, giving rise to a full spectrum of strong to fragile glass-forming behaviors. We have observed the dependence of particle motions and structural relaxation on particle volume fraction can be weakened by decreasing particle elasticity, due to particle deformation and the resulting interparticle elastic interaction upon intimate particle contacts at high particle concentration. Both measured α-relaxation time scales and dynamic length scales for cooperative rearranging motions of microgels in suspensions show similarly dependence on particle volume fraction and elasticity, thereby quantifying the glass fragility of dense microgel suspension of varied particle elasticity.

Glass-forming liquids are ubiquitous in nature and technology. Their dynamics and viscoelastic properties play a significant role in diverse applications from coating, lubrication, to polymer nanoimprinting. The glass transition remains to be one of the most contentious topics in complex fluids and condensed matter physics. [1-3] Upon approaching the glass transition, the viscosity (η) and relaxation time of a glass-forming liquid can grow by many orders of magnitude while the order of control parameters, such as T,[4-7] volume fraction, ϕ,[8] or film thickness by spatial confinement,[9] only changes by a factor of 1-2. However, the problem is incredibly more complex than the viscosity enhancement as arrays of glass formers display surprisingly diverse behaviors upon approaching the glass transition temperature, T_g that itself is difficult to define. [1] *Fragile* glass formers, such as ortho-terphenyl, polystyrene (PS), and poly(methyl methacrylate) (PMMA), show a steep super-Arrhenius increase with decreasing temperature while *strong* glass formers, such as silica, show only an Arrhenius increase. [10] A fragility index, m, defined as $m = d\log\eta/d(T_g/T)$, [10] has been introduced as a unifying concept to describe the glassy behaviors across various glass-forming liquids. Strong glass formers have low values of m, implying the change of viscosity with temperature is very modest as T_g is approached from above. In contrast, fragile glass formers have high values of m, indicating that the change of viscosity is steep for a modest reduction in temperature. Most polymeric materials and organic liquids fall into the category of fragile glass formers. [11] It is recently demonstrated that the fragility of glass formers can be tuned by adding substituents or increasing density.[7,12-13] For instance, PMMA has a fragility index of $m = 80$; when adding a cyclohexane ring as a substituent to make poly(cyclohexyl methacrylate), m is reduced by a factor of three [14]. In addition, by increasing the pressure of the liquid, T_g can be extended to higher temperatures, which will further modify the fragility of the glass. [15] Recently, the ratio between the

activation enthalpy and energy has been found to determine the fragility of the glass, yet there is limited adequacy of this relationship. [16] Further, a unique feature that contrasts strong glasses from fragile ones is that strong glasses possess highly directional bonding, resulting in anisotropic interaction potentials. [1,17] Yet, it is unclear how such directional interaction affects the process of microscopic structural relaxation.

Despite extensive experimental and theoretical investigations, the relaxation dynamics of glass forming liquids remains inadequately understood [2-5]. The Adam-Gibbs theory (AGT) proposed an entropic-driven relaxation process for glass formers and attributed the viscosity growth to the presence of dynamically heterogeneous sub-regions designated as "cooperatively rearranging regions" (CRRs). [8] The growth of the length scale associated with CRRs implies a random first-order transition (RFOT) from a liquid state to a glass state. [18-19] However, the AGT gives no explicit description of the structural relaxation for glass formers of different m or how the CRRs grow in strong glasses. Furthermore, while recent work using the AGT developed a highly specific relationship for the configurational entropy of the glassy material, a single equation detailing the slow-down dynamics for an arbitrary glass may not exist. [20] A similar dilemma is encountered with the mode-coupling theory (MCT) [12]. The MCT described the glass transition as the structural arrest of particles by the "cages" generated by their nearest neighbors and predicted the β- and α-relaxation times corresponding to the ballistic motion inside their cages and the long time scales for cage escaping, respectively. For molecular liquids, this model is only valid for low viscosity and diverges in the low temperature, ultra-viscous domain. [21] While these theories have been tested with both molecular and colloidal fragile glass formers to show good agreement with experimental [22] and computational results, [23] little insight is offered to the underlying physics responsible for the origin of glass fragility. There are

very few direct microscopic details of colloidal glasses to elucidate the relationship between heterogeneous dynamics and intermittent glass fragility.

Dense colloidal liquids have been examined by microscopy to reveal ϕ-dependent dynamic characteristics similar to the T-dependent behaviors of molecular glasses. [2,24-25] Colloidal liquids present an ideal system to study glassy dynamics over molecular glasses as the particles in a dense suspension are directly observable via optical microscopy and their dynamics is measurable in real time and real space. Therefore, this study focuses on colloidal glasses of tunable fragility and varied volume fraction to further elucidate the phenomena of glassy dynamics. Extensive microscopic studies on model "hard-sphere" colloidal liquids have confirmed the slow-down of particle motion in the super-cool region starting at $\phi \approx 0.53$ and the onset of the glass region at $\phi_g \approx 0.58$. [11,24-25] Yet, until recently, most colloidal systems are regarded as fragile glass formers. Highly deformable particles in liquid suspensions are demonstrated to make strong glasses, exhibiting a delayed onset of a glass state due to their elastic interparticle interactions. [11,26-27] However, a direct and quantitative study of glassy dynamics in a full range of m has been very few. [28] Distinct from previous studies which inferred glassy dynamics from dynamic light scattering and rheology measurements, [8,27] in this paper, we report the real-space and real-time microscopic study of the glassy dynamics in a single microgel system with varied particle elasticity, allowing us to tune fragility and examine its effect on structural relaxation. We tracked individual particle motions and analyzed structural relaxation of deformable microgel particles in aqueous suspensions of increased particle concentration toward the glass transition. We thus examined the relationship between particle elasticity, glass fragility, and structural relaxation of dense microgel suspensions.

Poly(N-isopropylacrylamide) (PNIPAM) microgels of varied crosslinking densities were synthesized using the method of free radical polymerization described elsewhere [29] and detailed in supplemental materials. Fluorescence-labeled PNIPAM microgels of five different crosslinker-to-monomer (CL) ratios of CL=0.9%, 1.6%, 2.2%, 3.3%, and 6.6% to vary the particle elasticity ranging from soft to model "hard" spheres were examined. Particle dynamics of PNIPAM microgel in bulk suspensions of volume thickness ≥ 150 μm were examined by three-dimensional visualization using a confocal laser scanning microscope (CLSM) (Zeiss LSM 5 Pascal) with an oil-immersion objective lens (*NA* = 1.4, 100x).

For non-"hard-sphere" colloidal suspension, ϕ-dependent phase behavior has not been explicitly defined and could strongly depend on particle elasticity. In this work, we have chosen ϕ ranging from the liquid regime to the values far exceeding the random close packing limit of ϕ=0.64 predicted for model "hard-sphere" suspensions. [8, 18] At all the ϕ studied in this work, microgel particles in aqueous suspensions exhibit disordered and amorphous static structures as confirmed by the Voronoi tessellation analysis (see Supplemental Figure 1). Considering the deformability of microgel particles upon intimate particle contact at high concentrations, we define the effective average radius, r_{eff}, of a microgel particle by the geometric mean of the unperturbed particle hydrodynamic diameter, d_H, and the center-to-center interparticle distance R_o, determined from the peak value of the pair correlation function, *g(r)* in Supplemental Figure 2, as $r_{eff} = \frac{1}{2}\sqrt{R_0 d_H}$. Accordingly, the effective volume fraction is defined as $\phi_{eff} = n \cdot \frac{\left(\frac{4}{3}\pi {r_{eff}}^3\right)}{V}$, where n is the total number of particles tracked in the box volume, *V*. As R_0 and d_H underestimates and overestimates the size of the microgel, respectively, there is a degree of error associated with r_{eff} and ϕ_{eff}. However, our ϕ_{eff} is consistent with the ones determined from the scaling of suspension viscosity with particle concentration. [27-28] Therefore, we expect the

values of r_{eff} and ϕ_{eff} are within acceptable degree of error for this study. We have observed that the primary peak in *g(r)* for PNIPAM particles of low CL=0.9 and 2.2 % shifts to smaller *r* with increased ϕ_{eff}, in sharp contrast to the ϕ_{eff}-independent, stable peak position for particles of CL=6.6 % that resemble "hard-sphere" colloids and $\phi_{eff} = \phi$ (see Supplemental Figure 2). Using a simple Hertzian model, [26] the elastic modulus, *E* (unit: Pa) of these microgel particles is estimated from *g(r)* following $U(r) = -k_B T lng(r) = \frac{4}{15} E(1 - \frac{r}{\sigma})^{5/2} V_c$ at $r \leq \sigma = 2r_{eff}$, where U(r) is the chemical potential energy, r is the radial distance from center of the particle, and V_c is the volume of the contact area and approximated as $V_c \approx \frac{4}{3}\pi(\frac{d_H - R_0}{2})^3$, and averaged over the values at different ϕ_{eff}. This model is valid for single contact between any two adjacent particles and therefore applicable for an intermediate concentration range as explored in this work. *E* of PNIPAM particles corresponding with varied CL is summarized in Table 1.

We start with measuring the mobility of PNINPAM particles of different *E* in aqueous suspensions against ϕ_{eff}. The particle mobility is quantified by the mean squared displacement (MSD) along the x-coordinate direction against lag time, τ [31-32]

$$< \Delta x^2 >= \frac{1}{N} \sum_{j=1}^{N} < [x_j(t) - x_j(\tau)]^2 > \quad \text{(Eq.1)},$$

which is averaged over all the N particles in the scan area and initial time, *t*. We did not analyze the MSDs along the z direction due to insufficient temporal resolution, which has been typically neglected in previous studies of particle dynamics using confocal microscopy. [9, 24, 31] On the other hand, the resolution in the x and y directions is equivalent and therefore $< \Delta x^2 > \approx < \Delta y^2 >$. Due to the size difference in the microgels of different *E*, we have normalized τ by a scaling factor, $k = \frac{d_{H,CL}}{d_{H,CL=6.6\%}}$, the size ratio of particle at CL=6.6% to the ones at different CL. For the stiffest microgel of E=2.6×10^4 Pa whose elasticity is comparable to that of common

microgels, [27,33] a strong dependence of MSD on ϕ_{eff} is observed in Figure 1c, exhibiting the characteristic "super-cooled" dynamics. As ϕ_{eff} increases, the mobility of particle decreases and becomes arrested at ϕ_{eff}=0.58, the same as the predicted for model "hard sphere" colloidal glass transition. [25] In contrast, for the softest PNIPAM particles of E=166 Pa, minimal change in mobility is observed in Figure 1 as increasing ϕ_{eff} from 0.49 to 0.61. At ϕ_{eff} =0.74 and 0.82, arrested particle motion is observed with the emerging plateau in MSD, where particles become caged by their neighbors over long timescales, and followed by sub-diffusive motion at $\tau > 5\times10^3$ sec due to cage escape. The weak dependence of MSD on ϕ_{eff} reflects the characteristics of non-fragile liquid behavior. For the PNIPAM particles of intermediate E=179 Pa, the dynamic behavior shown in Figure 1b falls between the "hard-sphere" and the soft ones. Substantial reduction in particle mobility is observed as increasing ϕ_{eff} from 0.38 to 0.61, yet the onset of an arrested state is measured at much higher concentrations, ϕ_{eff} =0.79. Furthermore, the plateau at intermediate ϕ_{eff} =0.61-0.68 is surprisingly short, suggesting caging is not fully enhanced. This is likely due to the deformation of particles upon intimate contact with their neighbors, which may facilitate the cage escape for structural relaxation.

Results shown in Figure 1 indicate that the onset ϕ_{eff} for dynamic arrest strongly depends on microgel elasticity. We then examine the E-dependent structural relaxation by measuring the overlap order parameter,

$$q_s(\tau) = \frac{1}{N}\sum_{i=1}^{N} w(|r_i(\tau) - r_I(0)|) \quad \text{(Eq. 2)},$$

where $w = 1\ or\ 0\ if\ |r_i(\tau) - r_i(0)| < or > a$, respectively. $q_s(\tau)$ quantifies the average number of "overlapping" particles separated by a distance, a, over a given τ, thereby evaluating the localization of particles. The parameter, a, is a "coarse graining" length scale that is typically larger than the vibration amplitude of particle motion in the β-regime. For "hard-sphere"

colloidal glasses, the particle radius is often chosen as a to give the best distinction between localized and delocalized particles. [9] In this work, considering the deformation of particles at high ϕ_{eff}, we have taken a = r_{eff} for the analysis. For PNIPAM particles of E=179 and 2.6×10^4 Pa as shown in Figure 1e-f, respectively, we have observed the glassy dynamics: $q_s(\tau)$ remains the unity at $\phi_{eff} \geq$ 0.61 and 0.51, respectively, where the particles are deeply localized over τ approaching 10^5 sec. In contrast, the softest PNIPAM particles of E=166 Pa become localized over much shorter τ from 10^3 sec to 4×10^4 sec at ϕ_{eff} =0.66-0.82, respectively. The α-relaxation time, τ_α, characterizing the super-exponential decay of q_s(τ), is extracted by fitting q_s(τ) with the Kohlrausch-Williams-Watts (KWW) formula, [33]

$$q_s(\tau) = Aexp(-(\tau/\tau_\alpha)^\beta) \quad \text{(Eq. 3)},$$

where A is a freely floating parameter for varied ϕ_{eff} and E and β is the stretching exponent. τ_α as a function of ϕ_{eff} for PNIPAM microgel of different E is summarized in Figure 2. Within a degree of error associated with this fitting procedure, two contrasting behaviors of τ_α are apparent. Softer microgel particles exhibit a gradual growth of τ_α with ϕ_{eff} while there is a much more abrupt, Super-Arrhenius growth for the stiffer microgel particles. The dependence of τ_α on E suggests that the MCT can be applied to strong glass-forming liquids. β against ϕ_{eff}/ϕ_g for PNIPAM microgel of different E is summarized in Supplemental Figure 3. As expected, the relaxation stretches with increasing ϕ_{eff} through the super-cooled phase approaching the glass transition. Interestingly, the relaxation becomes more stretched at smaller volume fractions for the softer microgel, providing further evidence of the E dependence of the microgel phase behavior.

We have determined the phase diagram from τ_α for non-"hard-sphere" PNIPAM microgels of different E in Figure 3. A *liquid* phase is characterized by a simple exponential decay of $q_s(\tau)$ without noticeable dynamic arrest. A *glass* phase is defined by $\tau_\alpha \geq \tau_g$, where $\tau_g=10^5$ sec is chosen as it recovers the onset volume fraction, ϕ_g=0.58 for the stiffest PNIPAM microgel resembling "hard-sphere" colloids. [11] ϕ_g for non-"hard-sphere" PNIPAM particles is determined by interpolating ϕ_{eff} at $\tau_\alpha=\tau_g$. The intermediate *super-cooled* phase between the *liquid* and *glass* states exhibits significant slow-down of particle dynamics with $\tau_\alpha<\tau_g$. Representative micrographs at each phase for PNIPAM microgels of E=166 and 2.6×10^4 Pa are exhibited in Supplemental Figure 4. For the particles of E= 436 and 2.6×10^4 Pa, their phase diagrams appear similar to ones reported for "hard-sphere" colloids, where the glass transition is determined at ϕ_g =0.58. Decreasing E leads to an extended super-cooled regime and shifts the ϕ_g to higher ϕ_{eff}, indicating a much more gradual transition as specified in the plot of $k\tau_\alpha$ against ϕ_{eff}/ϕ_g in Figure 2. In agreement with the AGT, τ_α is observed to scale as $e^{A/\phi_{eff}}$, where A is a constant related to configurational entropy. For the two stiffest microgels, there is a sharp increase in τ_α as the glass transition is approached. For soft microgels of E=166-179 Pa, the increase of τ_α with ϕ_{eff} becomes much more gradual, exhibiting the characteristic of strong glass formers. We thus determine the fragility index, m, from the results of τ_α shown in Figure 2 as $m_\tau = \left[\frac{d[\ln(\tau_\alpha)]}{d(\phi/\phi_g)}\right]_{\phi=\phi_g}$ (Eq. 4) and plotted against E in Figure 5. The stiffest microgels show the highest index value of $m_\tau \approx 10$, which agrees with the value reported for model "hard-sphere" colloidal glass. [35] m_τ decreases sharply to ≈4 for the two softest microgel systems. This behavior is similar to molecular glasses where the fragility index drops precipitously from 80 for PMMA fragile glass to 20 for SiO_2 strong glass. [10] We also observe the presence of an intermediate regime at intermediate E,

which does not fall into either strong or fragile glass former groups as described in the Angell's plot. [4] Nevertheless, it suggests that tuning particle elasticity, giving rise to varying interparticle elastic interaction, could cause the transition between strong and fragile glasses.

Results shown in Figure 1 and 2 also suggest that highly deformable microgel particles are less caged even at volume fractions beyond close packing. Thus, we expect that decreasing particle elasticity enhances the cooperative motion responsible for the structural relaxation. We have quantified the CRRs by the correlation length scales using the four-point correlation function, $g_4(r,\tau)$ of the dynamics measured in two different points of time and space:

$$g_4(r,\tau) = \frac{1}{N\rho}\sum_{ijkl} < \delta\big(r + r_k(0) + r_i(0)\big) \cdot w\left(r_i(0) - r_j(\tau)\right) \cdot w\big(r_k(0) - r_l(\tau)\big) > - < \frac{q_s(\tau)}{N} >^2 \quad \text{(Eq. 5)}$$

where the first term is a pair correlation function, $g_4^{ol}(r,\tau)$ for overlapping particles and the second term is the square mean value of $q_s(\tau)$ in Eq. 2. We have calculated

$$g_4{}^*(r,\tau) = g_4^{ol}(r,\tau)/< q_s(\tau)/N >^2 - 1 \quad \text{(Eq. 6)}$$

and shown $g_4{}^*(r,\tau)$ at varied τ and ϕ_{eff} for PNIPAM microgel of varied E in Supplemental Figure 5. Consistent with our prior work [9], we have confirmed that $g_4{}^*(r,\tau)$ captures the dynamic heterogeneity of the stiffest PNIPAM microgels where the range of dynamic correlations reaches a maximum at an intermediate time scale and decrease at shorter and longer time scales. Surprisingly, for soft microgel particles, $g_4{}^*(r,\tau)$ do not show any growth over the observation period. We have applied an "envelop fitting" method to extract the dynamic length scale, ξ_4, on the time scales where $g_4{}^*(r,\tau)$ is peaked using $g_4{}^*(r,\tau) = Aexp(-r/\xi_4)$ over a range of 2 μm < r < 9 μm where A is a free floating variable. [9,36-37] ξ_4 is a time-dependent property that reveals the growth of CRRs in the super-cooled regime. We have observed the presence of a characteristic peak in ξ_4 at long lag times for both the softest and stiffness microgels as shown in Figure 4a-b, respectively. It suggests that the growth of CRRs to their maximum sizes is a slow

process that could be independent of liquid fragility. Consistent with our previous observations, [9] we have observed the largest ξ_4 with the stiffest microgel of E=2.6×10^4 Pa as shown in Figure 4b. The peak values of ξ_4 are typically considered the equilibrium sizes of the CRR, [9] shown as a function of E in the inset of Figure 4c. Consistent with the behavior of $g_4^*(r,\tau)$, ξ_4 does not significantly vary for the softer microgels and increases abruptly for the stiffer microgels. The maximum ξ_4, normalized by $\xi_{4,glass}$ at ϕ_{eff} is plotted against ϕ_{eff}/ϕ_g in Figure 4c. Evidently, the growth of ξ_4 with ϕ_{eff} is much more gradually for the microgels of lower E. Although the AGT did not explicitly predict how the CRRs grow in strong glass former, the results shown in Figure 4 suggest a similar process for the fragile and strong glass-forming liquids. The extended super-cooled phase for the softer microgels likely leads to the gradual growth of CRRs, where the abrupt growth CRRs observed for stiff microgels results from the small super-cooled phase. We have also derived the fragility index from ξ_4 as $m_\xi = \left[\frac{d\xi_4}{d(\phi/\phi_g)}\right]_{\phi=\phi_g}$ (Eq. 7). As shown in Figure 5, the striking similarity between m_τ and m_ξ and their dependence on E provide direct evidence of the strong relationship between cooperative motions and glass fragility.

In conclusion, we have examined the transition between strong and fragile glass formers in a single microgel system of varied particle elasticity. PNIPAM microgel particles of high elasticity resemble the model "hard-sphere" colloidal liquids as fragile glass formers, where both τ_α and ξ_4 show a super-Arrhenius increase with ϕ_{eff}. Highly deformable microgel particles of decreasing elasticity exhibit a delayed glass transition at higher ϕ_{eff} and an extended super-cooled regime. The dependence of τ_α and ξ_4 on ϕ_{eff} is weakened by lowering elasticity, leading to the transition from fragile to strong glasses. This is further revealed by the elasticity dependence of the fragility indices, m_τ and m_ξ. It suggests that the glass fragility and structural relaxation

processes of glass-forming liquids can be modified by particle elasticity due to particle deformation that gives rise to enhanced elastic interaction between particles.

Acknowledgements.

This work is supported by the National Science Foundation (NSF) (CMMI 100429 and 1129821). R.P.S acknowledges the financial support from NSF EAPSI fellowship program for international research collaboration and travel. Z. Z. acknowledges the financial supported by the National Natural Science Foundation of China (21174101 and 2012CB821500) and the Project for Jiangsu Scientific and Technological Innovation Team (2013).

References

[1] M. D. Ediger, Spatially Heterogeneous Dynamics in Supercooled Liquids. *Annu. Rev. Phys. Chem.* **2000**, *51*, 99-128.

[2] E. R. Weeks, J. C. Crocker, A.C. Levitt, A. Schofield, and D.A. Weitz, Three-Dimensional Direct Imaging of Structural Relaxation near the Colloidal Glass Transition. *Science* **2000,** *287*, 627-631.

[3] W. Härtl, Colloidal Glasses. *Current Opinion Colloid & Interface Sci.* **2001**, *6*, 479-483.

[4] C. A. Angell, Formation of Glasses from Liquids and Biopolymers. *Science* **1995**, *267*, 1924-1935.

[5] K. Ito, C. T. Moynihan, and C. A. Angell, Thermodynamic Determination of Fragility in Liquids and A Fragile-to-Strong Liquid Transition in Water. *Nature* **1999**, *398,* 492-495.

[6] C. A. Angell, K. L. Ngai, G. B. McKenna, P. F. McMillan, and S. W. Martin, Relaxation in Glassforming Liquids and Amorphous Solids. *J. Appl. Phys.* **2000**, *88*, 3113.

[7] H. Lindsay and P. Chaikin, Elastic Properties of Colloidal Crystals and Glasses. *J. Chem. Phys.* **1982,** *76*, 3774-3781.

[8] P. Segre, S. Meeker, P. Pusey, and W. Poon, Viscosity and Structural Relaxation in Suspensions of Hard-Sphere Colloids. *Phys. Rev. Lett.* **1995**, 75, 958.

[9] P. S. Sarangapani, A. B. Schofield, and Y. Zhu, Direct Experimental Evidence of Growing Dynamic Length Scales in Confined Colloidal Liquids. *Phys. Rev. E* **2011**, *83,* 030502.

[10] R. Böhmer, K. L. Ngai, C. A. Angell, and D. J. Plazek, Nonexponential Relaxations in Strong and Fragile Glass Formers. *J. Chem. Phys.* **1993**, *99,* 4201-4209.

[11] P. G. Debenedetti and F. H. Stillinger, Supercooled Liquids and the Glass Transition, *Nature* **2001**, *410,* 259-267.

[12] R. Richert, Geometrical Confinement and Cooperativity in Supercooled Liquids Studied by Solvation Dynamics. *Phys. Rev. B* **1996**, *54,* 15762.

[13] R. A. Riggleman, K. Yoshimoto, J. F. Douglas, and J. J. de Pablo, Influence of Confinement on the Fragility of Antiplasticized and Pure Polymer Films. *Phys. Rev. Lett.* **2006**, *97,* 045502.

[14] K. Kunal, C. G. Robertson, S. Pawlus, S. F. Hahn, and A. P. Sokolov, Role of Chemical Structure in Fragility of Polymers: A Qualitative Picture. *Macromolecules* **2008**, *41,* 7232-7238.

[15] T. Atake and C. A. Angell, Pressure dependence of the glass transition temperature in molecular liquids and plastic crystals. *J. Phys. Chem.* **1979**, 83, 3218-3223.

[16] J. C. Martinez-Garcia, S. J. Rzoska, A. Drozd-Rzoska, S. Starzonek, and J. C. Mauro, Fragility and basic process energies in vitrifying systems. *Nature Scientific Reports* **2015**, *5*, 1-7.

[17] K. Binder and W. Kob, *Glassy materials and disordered solids: An introduction to their statistical mechanics* (World Scientific 2011).

[18] T. Kirkpatrick, D. Thirumalai, and P. G. Wolynes, Scaling Concepts for the Dynamics of Viscous Liquids near an Ideal Glassy State. *Phys. Rev. A* **1989**, *40,*1045.

[19] V. Lubchenko and P. G. Wolynes, Theory of Structural Glasses and Supercooled Liquids. *Annu. Rev. Phys. Chem.* **2007**, *58,* 235-266.

[20] J. C. Martinez-Garcia, S. J. Rzoska, A. Drozd-Rzoska, and J. Martinez-Garcia, A universal description of ultraslow glass dynamics. *Nature Communications* **2013***, 4*, 1823

[21] C. A. Angell, Perspective on the glass transition, *J. Phys. Chem. Solids* **1988**, *48*, 863-871

[22] W. Van Megen and S. Underwood, Glass Transition in Colloidal Hard Spheres: Measurement and Mode-Coupling-Theory Analysis of the Coherent Intermediate Scattering Function. *Phys. Rev. E* **1994**, *49,* 4206.

[23] W. Kob and H. C. Andersen, Testing Mode-Coupling Theory for a Supercooled Binary Lennard-Jones Mixture I: The van Hove Correlation Function. *Phys. Rev. E* **1995**, *51,* 4626.

[24] E. R. Weeks and D. Weitz, Properties of Cage Rearrangements Observed near the Colloidal Glass Transition. *Phys. Rev. Lett.* **2002**, *89,* 095704.

[25] P. Pusey and W. Van Megen, Phase Behaviors of Concentrated Suspensions of Nearly Hard Colloidal Spheres. *Nature* **1986**, *320,* 340-342.

[26] A. J. Liu and S. R. Nagel, *Jamming and rheology: constrained dynamics on microscopic and macroscopic scales* (CRC Press, 2001).

[27] J. Mattsson, H. M. Wyss, A. Fernandez-Nieves, K. Miyazaki, Z. Hu, D. R. Reichman, and D.A. Weitz, Soft Colloids Make Strong Glasses. *Nature* **2009**, *462,* 83-86.

[28] Y. Rahmani, K. van der Vaart, B. van Dam, Z. Hu, V. Chikkadi, and P. Schall, Dynamic Heterogeneity in Hard and Soft Sphere Colloidal Glasses. *Soft Matter* **2012**, *8,* 4264-4270.

[29] R. Pelton and P. Chibante, Preparation of Aqueous Lattices with N-isopropylacrylamide. *Colloids Surf.* **1986**, *20,* 247-256.

[30] J. Yang and K. S. Schweizer, Glassy Dynamics and Mechanical Response in Dense Fluids of Soft Repulsive Spheres. I. Activated Relaxation, Kinetic Vitrification, and Fragility. *J. Chem. Phys.* **2011**, *134,* 204908..

[31] Our analysis shows that $\langle x^2 \rangle \approx \langle y^2 \rangle$, which is not shown here. Because of slower scanning along the z-direction, we focus on the in-plane particle dynamics parallel to the confining walls (the xy plane) in this work.

[32] R. Yamamoto and A. Onuki, Dynamics of Highly Supercooled Liquids: Heterogeneity, Rheology, and Diffusion. *Phys. Rev. E* **1998**, *58*3515.

[33] J. J. Liétor-Santos, B. Sierra-Martín, and A. Fernández-Nieves, Bulk and Shear Moduli of Compressed Microgel Suspensions. *Phys. Rev. E* **2011**, *84,* 060402.

[34] P. S. Sarangapani, A. B. Schofield, and Y. Zhu, Relationship between Cooperative Motion and the Confinement Length Scale in Confined Colloidal Liquids. *Soft Matt.* **2012**, *8,* 814-818.

[35] G. Brambilla, D. Brambilla, M. El Masri, L. Pierno, L. Berthier, G. Cipelletti, A. Petekidis, and Schofield, Probing the Equilibrium Dynamics of Colloidal Hard Spheres above the Mode-Coupling Glass Transition. *Phys. Rev. Lett.* **2009**, *102,* 085703.

[36] N. Lačević, F. W. Starr, T. Schrøder, and S. Glotzer, Spatially Heterogeneous Dynamics Investigated via a Time-Dependent Four Point Density Correlation Function. *J. Chem. Phys.* **2003**,119, 7372.

[37] P. Ballesta, A. Duri, and L. Cipelletti, Unexpected Drop of Dynamical Heterogeneities in Colloidal Suspensions Approaching the Jamming Transition. *Nature Physics* **2008**, *4,* 550-554.

Table 1. Materials properties of PNIPAM microgel particles of different crosslinking density (CL) that leads to varied hydrodynamic diameter (d_H), elastic modulus (E), scaling factor (k), and onset volume fraction for glass transition (ϕ_g). ϕ_g for non-"hard-sphere" PNIPAM particles of different E is determined by interpolating ϕ_{eff} at $\tau_\alpha=\tau_g$.

CL (%)	0.9	1.6	2.2	3.3	6.6
d_H (μm)	1.77	1.34	1.95	1.85	1.4
E (Pa)	166±106	169±24	179±34	436±24	(2.6±1.5)×10^4
k	2.02	0.88	2.70	2.31	1
ϕ_g	0.96	0.87	0.72	0.58	0.58

Figure caption

Figure 1. Mean-squared displacements (MSD) plotted against scaled lag time, $k\tau$, for dense PNIPAM microgels of (a) E = 166 Pa at ϕ_{eff} = 0.49 (black squares), 0.54 (red circles), 0.61 (green triangles), 0.66 (inverted blue triangles), 0.74 (cyan diamonds) and 0.82 (magenta left-facing triangle), (b) E = 179 Pa at ϕ_{eff} = 0.38 (black squares), 0.51 (red circles), 0.61 (green triangles), 0.68 (inverted blue triangles), and 0.79 (cyan diamonds), and (c) E = 2.6×10^4 Pa at ϕ_{eff} = 0.38 (black squares), 0.48 (red circles), 0.51 (green triangles), 0.56 (inverted blue triangles) and 0.58 (cyan diamonds). (d)-(f) Overlap order parameter, $q_s(\tau)$, corresponding to PNIPAM microgels shown in (a)-(c), respectively, with the same symbol colors and shapes.

Figure 2. Scaled α-relaxation time, $k\tau_\alpha$, is plotted against ϕ_{eff} normalized by ϕ_g for PNIPAM microgels of E = 166 Pa (black squares), 169 Pa (red circles), 179 Pa (green triangles), 436 Pa (inverted blue triangles), and 2.6×10^4 Pa (cyan diamonds). Solid lines represents the scaling of the data points with the Adam-Gibbs model, $\tau_\alpha \sim e^{A/\phi_{eff}}$ **Inset:** $k\tau_\alpha$ is plotted against ϕ_{eff}.

Figure 3. Phase diagram of PNIPAM microgels of different E versus ϕ_{eff}, exhibiting three distinct phases, *liquid* (black circles), *super-cooled* (red triangles), and *glass* (green inverted triangels.) Arrows and dash-lines are drawn as the guideline for eyes.

Figure 4. Dynamic length scale, ξ_4, scaled by corresponding r_{eff}, for PNIPAM particle of (a) E = 166 Pa at ϕ_{eff} = 0.47 (black squares), 0.60 (red circles), 0.75 (green triangles), and 0.81 (inverted blue triangles) and (b) E= 2.6×10^4 Pa at ϕ_{eff} = 0.49 (black squares), 0.52 (red circles), 0.56 (green triangles), and 0.58 (inverted blue triangles). (c) Normalized ξ_4 by the one upon the glass

transition, $\xi_{4,g}$, is plotted against ϕ_{eff}/ϕ_g for PNIPAM microgels of E = 166 Pa (black squares), 169 Pa (red circles), 179 Pa (green triangles), 436 Pa (inverted blue triangles), and 2.6×10^4 Pa (cyan diamonds). **Inset:** $\xi_4/\xi_{4,g}$ is plotted against ϕ_{eff}.

Figure 5. Fragility indices m_τ (black squares) and m_ξ (red circles) against E.

Figure 1

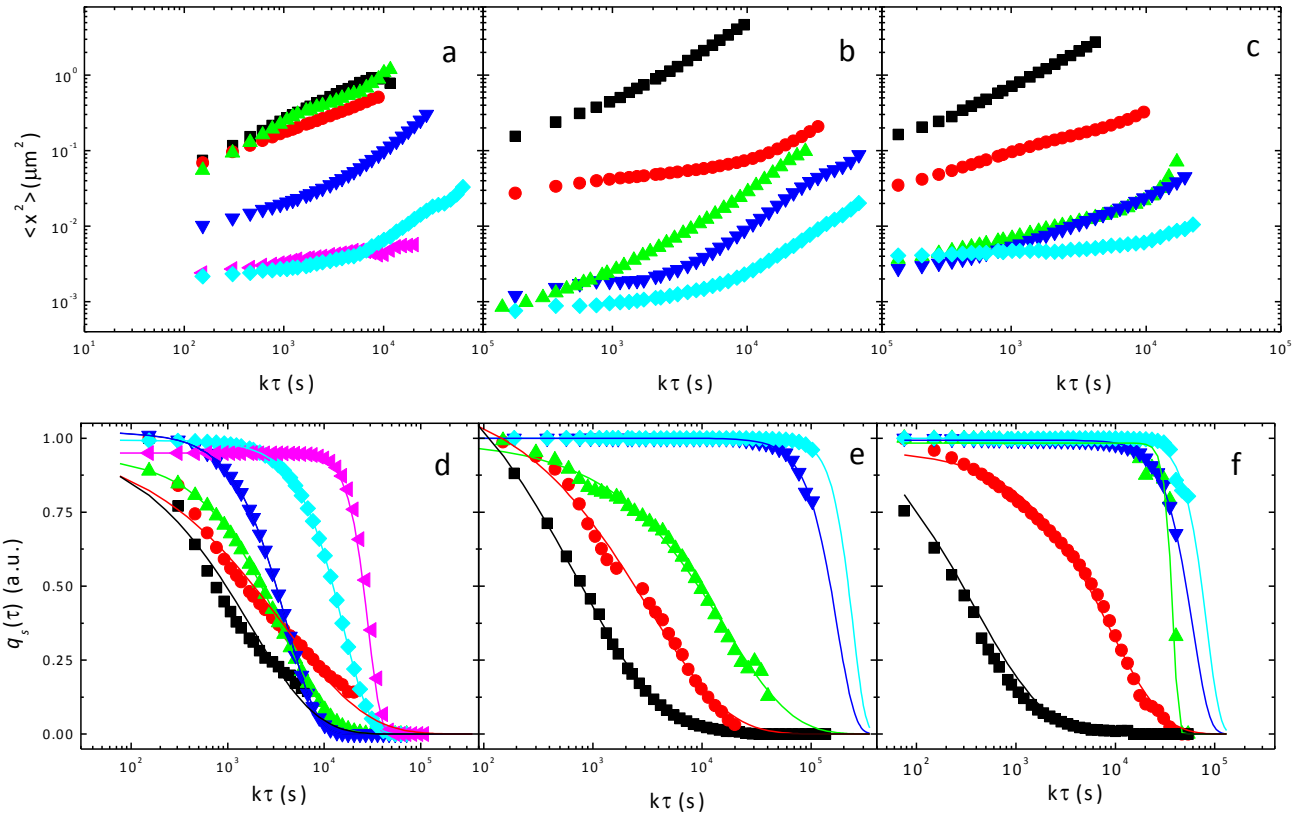

Figure 2

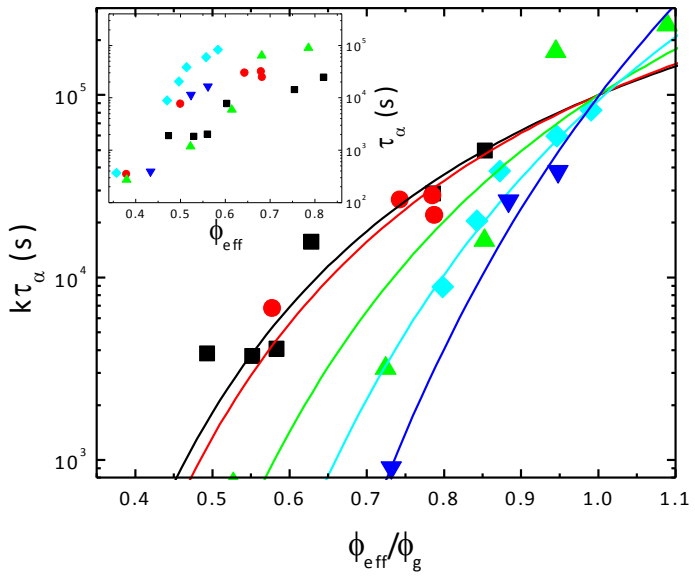

Figure 3

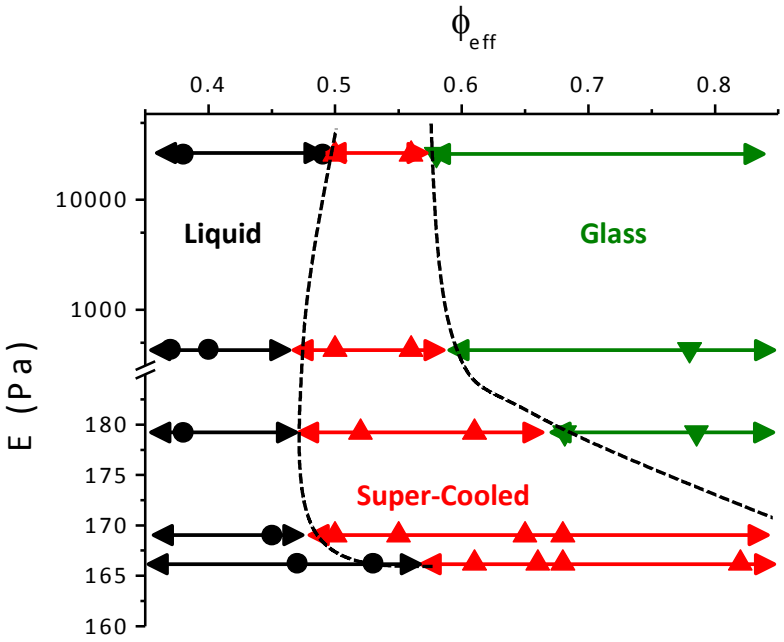

Figure 4

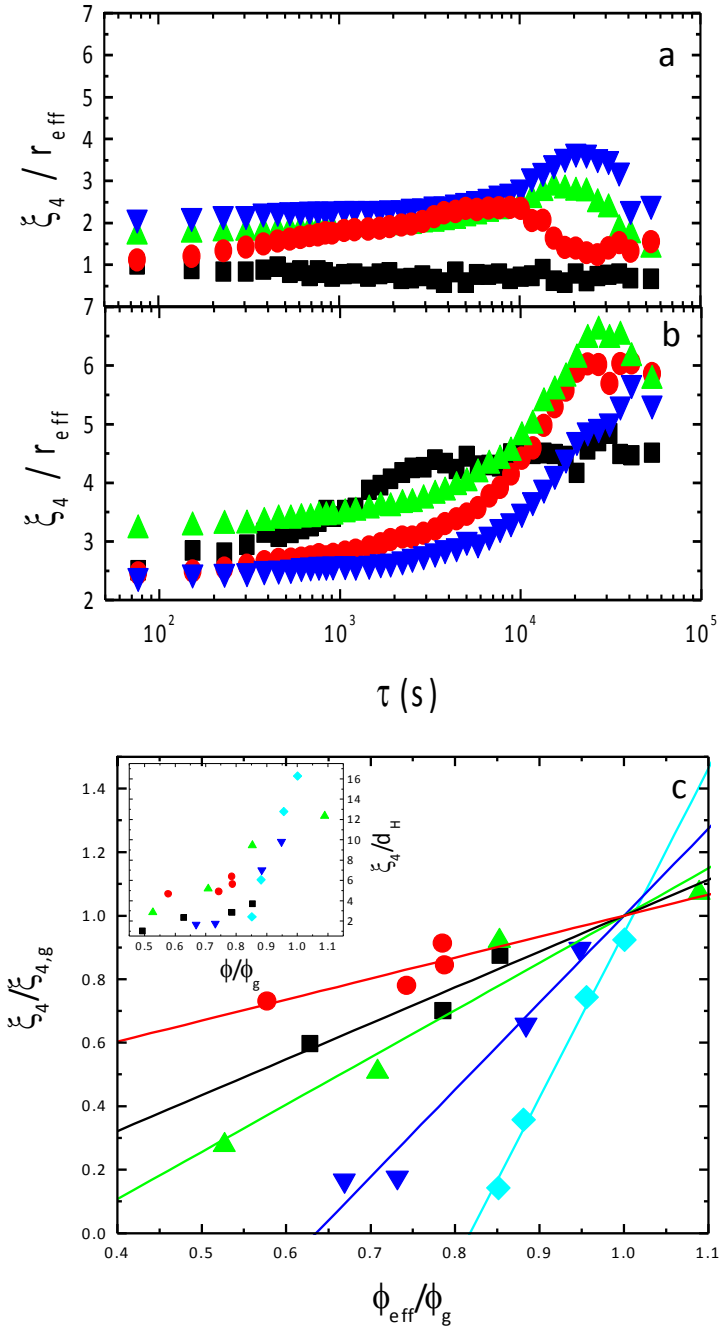

Figure 5

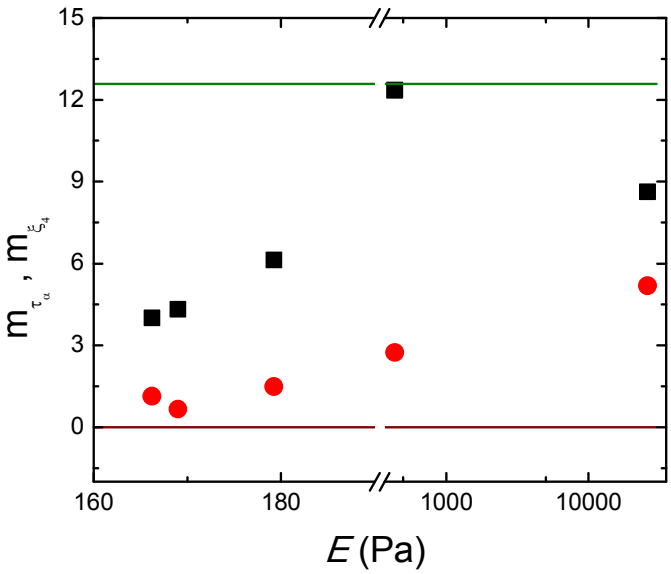

ToC Graphics